Locating Transverse Cracks in Prismatic Beams Using Random Forest Method and The Frequency Drop

Cristian TUFIȘI
Department of Engineering Science, Babes-Bolyai University, Str. M. Kogălniceanu 1, 400084 Cluj-Napoca, Romania, cristian.tufisi@ubbcluj.ro

Vasile-Catalin RUSU
Department of Computer Science, Institute of German Studies, Babeş-Bolyai University, Str. M. Kogălniceanu 1, 400084 Cluj-Napoca, Romania, vasile.rusu@ubbcluj.ro

Gilbert-Rainer GILLICH
Department of Engineering Science, Babes-Bolyai University, Str. M. Kogălniceanu 1, 400084 Cluj-Napoca, Romania, gilbert.gillich@ubbcluj.ro

Abstract: As the infrastructure ages and nears the end of its estimated operating time, the detection of damages becomes a major issue in structural health monitoring (SHM). In this paper, the authors propose an analytical approach for generating the data needed to train a Random Forest model (RF) that will perform the SHM task, namely, to detect, locate, and assess the severity of transverse cracks in beam-like structures. Using an original method, we calculate the relative frequency shifts (RFS) for different damage scenarios and use the generated data to train the RF model. Subsequently, the validation of the RF model is performed using data obtained from FEM simulations using different mesh sizes, for different damage scenarios on steel beams. The results indicate that the RF model can detect the presence of the defect and find the position and depth of the transverse cracks very precisely if the crack is located in the area where the beam achieves the maximum bending moment.

Keywords: - damage detection, transversal crack, decision trees, random forest, relative frequency shift

1. INTRODUCTION

As technology advances, new techniques have been developed in recent years to detect damages in structures. The developed methods allow real-time global monitoring of equipment or large structures by correlating damage characteristics such as depth and location with the changes of the dynamic parameters (eigenfrequencies, mode shapes) [1-3]. SHM involves the integration of sensors, intelligent data acquisition, transmission, and computational mechanisms in a new system, capable of locating, evaluating, and estimating the propagation of a crack inside a structure [4, 5]. SHM techniques can be successfully applied in the aerospace domain, in industrial manufacturing, or civil engineering [6]. The most common vibration-based damage detection method uses eigenfrequencies to observe and quantify structural changes [7]. Now, numerous scholars imply artificial intelligence to find the correlation between the structural and modal parameters. Neural networks [8-10] and particle swarm optimization [11, 12] are presently the most used methods to assess damage in different kinds of structures.

An example of using Random Forests (RF) for SHM is presented in [13]. The authors use a decision tree for detecting damages on several test models. An RF model was also used in [14] for analyzing the integrity of high-speed railway track slabs.

The method we propose here involves an analytical model that can predict the RFS caused by transverse cracks in beam-like structures. We create a dataset by generating different scenarios for a cantilever beam affected by cracks in the area where the biggest bending moments are achieved. The trained RF model was able to detect the location and severity of cracks with high precision.

2. GENERATING THE TRAINING DATA

It is known that when a crack occurs in a structure, it produces an alteration of the stiffness, which in return produces a change in the dynamic parameters. In prior articles, we proposed a robust and easy-to-use mathematical relation to calculate the eigen-frequencies $f_{i\text{-}D}(x,a)$ of a cracked beam [15]. The relation requires knowing the eigenfrequencies $f_{i\text{-}U}$ of the intact beam and the crack depth a and position x.

Table 1. Equations used for determining the decrease in natural frequencies

Parameter	Mathematical relation	Eq. number
Eigenfrequency of the damaged beam	$f_{i-D}(x,a) = f_{i-U}\left\{1-\gamma(a)\left[\bar{\phi}_i''(x)\right]^2\right\}$	(1)
The severity of a crack of known depth a	$\gamma(a) = \frac{\sqrt{\delta_D(a)} - \sqrt{\delta_U}}{\sqrt{\delta_D(a)}}$	(2)
Normalized modal curvature	$\bar{\phi}_i''(x) = 0.5\left\{\cos(\lambda_i x) + \cosh(\lambda_i x) - \frac{\cos\lambda_i + \cosh\lambda_i}{\sin\lambda_i + \sinh\lambda_i}\left[\sin(\lambda_i x) + \sinh(\lambda_i x)\right]\right\}$	(3)
Relative frequency shift	$\Delta\bar{f}_{i-D}(x,a) = \frac{f_{i-U} - f_{i-D}(x,a)}{f_{i-U}} = \gamma(a)\left[\bar{\phi}_i''(x)\right]^2$	(4)

Thus, besides the eigenfrequency of the intact beam, relation (1) includes the severity $\gamma(a)$ and the modal curvatures of the out-of-plain vibration modes $\phi_i''(x)$. While the modal curvature has a well-known relation, the crack severity is calculated after a methodology comprehensively described in [16, 17].

Finally, the relative frequency shift (RFS) is calculated with Eq. (4), as the normalized difference between the eigenfrequency of the intact beam and the eigenfrequency of the damaged beam [18]. All relations necessary to generate the training dataset are presented in Table 1.

In Figure 2 we exemplify the RFS calculated using Eq. (4) for vibration mode 5, in case of a transverse crack with the known depth extent of 20% relative to the total thickness of the beam.

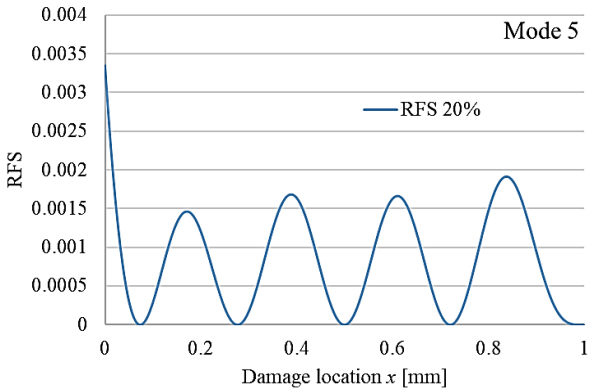

Figure 1. Plotted RFS function for out-of-plain bending vibration mode 5 of a cantilever beam

By using the above approach, we calculated the RFS values for the first eight bending weak-axis vibration modes for a cantilever beam that is affected by a transverse crack of different known depths and locations.

For the present study, we considered as possible locations of the crack only the area where the beam is subjected to a large bending moment, i.e. the first 100 mm from the fixed end. We limited the study to this area because it is most likely to be affected by the damage. The relative damage depth is taken between 10% to 62 %. The set of data consists of:

- INPUT – the first eight RFS values for a given crack position and severity;
- TARGET – the crack position and severity.

To determine the optimal amount of data necessary for obtaining an accurate RF model, we have considered four training cases. The considered variables for the four datasets are the resolution of the crack location along the beam (the distance between two consecutive crack positions) and the depth resolution (the percentage difference between two consecutive depths of the crack). Consequently, the following training cases resulted in:

Case 1: the RFS values are calculated with a crack position resolution of 10 mm and damage depths: 10%, 20%, 32%, 40%, 52%, and 60%.

Case 2: the RFS values are calculated with a crack position resolution of 10 mm and relative damage depths 10% to 62 % with a step of 4%.

Case 3: the RFS values are calculated with a damage position step of 2 mm and damage depths: 10%, 20%, 32%, 40%, 52%, and 60%.

Case 4: the RFS values are calculated with a damage position step of 2 mm and damage depths 10% to 62 % with a step of 4%.

By employing the 4 input datasets we train the four RF models and determine the precision for detecting the location of the crack for each one by involving RFS determined with numerical simulation performed in ANSYS.

3. THE RANDOM FOREST MODEL

Decision tree-based algorithms are popular machine learning methods used to solve supervised learning problems. These algorithms are flexible and can solve any problem at hand.

Random forest is one of the most popular supervised tree-based learning algorithms. It is also the most flexible and easy to use. The algorithm can be used to solve both classification and regression problems. The random forest tends to combine hundreds of decision trees and then employs each decision tree onto a different sample of observations.

The performance of a RF has been shown to depend on a few key hyper-parameters [19]. Table 2 shows the values for the hyper-parameters as used in this study. These values were obtained by using a randomized search with 5-fold-cross-validation, that randomly selects values for the hyper-parameters and scores the estimator at the end. The best estimator is used in this study. The ranges for all hyper-parameters used are shown in Table 3.

Table 2. RF hyper-parameters.

Parameter	Range
n_estimations	200-2000, step 200
max_depth	None; 10-110, step10
min_samples_split	2, 5, 10
min_samples_leaf	1, 2, 4
bootstrap	True, False

Table 3. Ranges for the RF hyper-parameters.

Parameter	Meaning	Value
n_estimations	The number of estimators in the forest	400
max_features	max number of features considered for splitting a node	sqrt
max_depth	max number of levels in each decision tree	None
min_samples_split	min number of data points placed in a node before the node is split	2
min_samples_leaf	min number of data points allowed in a leaf node	1
bootstrap	method for sampling data points. True= bootstrap samples	true

The training was performed for the generated datasets as described in the previous section. In consequence, four RF models are created, which we denote after the training dataset: RF1 for the dataset generated according to Case 1, RF2 for Case 2, RF3 for Case 3, and RF4 for Case 4.

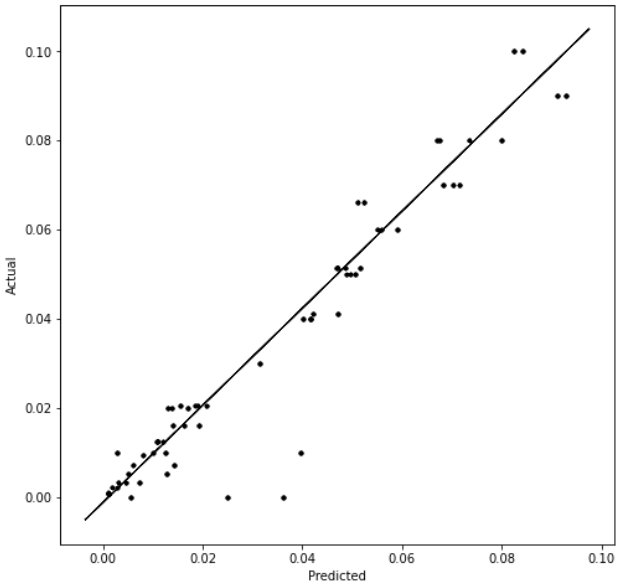

Figure 2. RF training results obtained for the training using the dataset with the least data (Case 1)

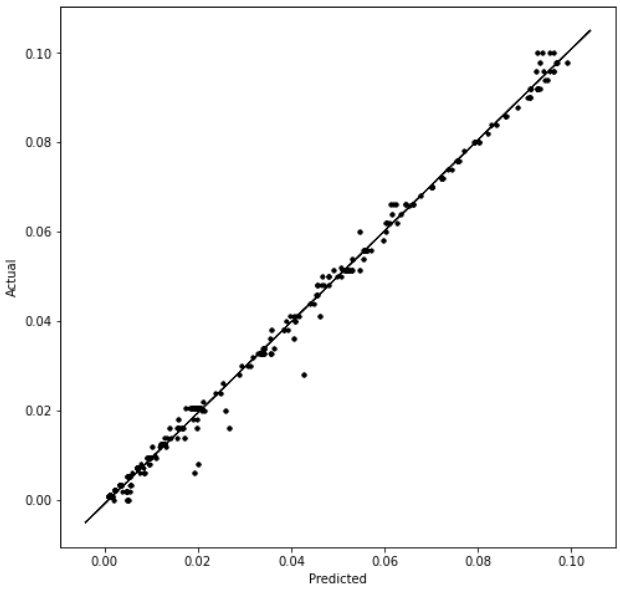

Figure 3. RF training results obtained for the training using the dataset with the most data (Case 4)

Figure 2 represents the training results for RF1, with the dataset having the least data, while Figure 3 represents the training results for RF4, with the dataset having the most data. The RF model trained with more data performs as expected better on the training set, with a mean squared error (MSE) of 0.005129 and an R^2 score of 0.9935. The model trained on the coarse dataset achieves a 0.07157 MSE and an R^2 score of 0.9117.

4. TEST DATA GENERATION

For testing the reliability of the four RF models for damage detection, we performed finite element

analysis using the modal tool integrated into the ANSYS software.

The beam geometry used for this study is generated using the design modeler with its main dimensions and structural steel material properties presented in Table 2.

Table 4. The beam's dimensions and material properties

Length L [mm]	Width B [mm]	Thickness H [mm]	Density [kg/m^3]	E [MPa]
1000	50	5	7850	$2 \cdot 10^{11}$

The beam is fixed at the left end, and the damage is modeled using a separate element by imposing the needed boundary conditions to replicate a transverse breathing crack. Thus, we ensure the same mass for the intact beams and the beams with transverse cracks, yet obtain the required discontinuities. A schematic of the beam is presented in Figure 4.

The FEM model is composed of the beam body and the parameterized elements used to create discontinuities; the bounded contact conditions are plotted with a blue dashed line, the free boundary with the red line, and the fixed end (transverse surface) with the green lines. We have considered for the simulation a mesh with hexahedral elements of 2mm maximum edge size for all the defined damage scenarios and, afterward, a more refined mesh having hexahedral elements of 1mm maximum edge size.

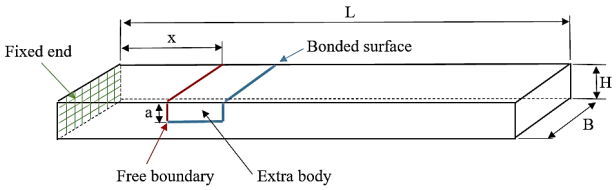

Figure 4. Schematic of the damaged cantilever beam

First, we obtain the eigenfrequencies for the intact beam for both mesh sizes. For testing the RF models we have considered diverse damage scenarios by variating the damage location between 0 and 100 mm along the beam. For all scenarios, the crack depth *a* is 1 mm. The damage scenarios used for testing the RF models are presented in Table 5 for mesh size 2 mm, and in Table 6 for mesh size 1 mm. The obtained RFS values are also indicated in these tables.

For demonstrating the effect that the mesh size has on the obtained FEM results, and also to compare the results with those for the analytical model, we plot in Figures 5-9 the RFS values for five relevant scenarios: one having the crack position close to the fixed end, three with intermediate positions, and one considering the crack close to the segment's end (i.e. near 100 mm taken from the clamped end).

Table 5. RFS for the mesh size 2 mm

Scenario	1a	2a	3a	4a	5a	6a	7a
Damage location	24 mm	30 mm	36 mm	56 mm	73 mm	88 mm	97 mm
RFS_1	0.00272	0.00262	0.00267	0.00247	0.00239	0.00224	0.00223
RFS_2	0.00228	0.00199	0.00214	0.00156	0.00127	0.00098	0.00086
RFS_3	0.00194	0.00152	0.00173	0.00094	0.00059	0.00031	0.00022
RFS_4	0.00159	0.00108	0.00132	0.00045	0.00014	0.00001	0.00001
RFS_5	0.00132	0.00075	0.00101	0.00017	0.00002	0.00009	0.00023
RFS_6	0.00103	0.00045	0.00071	0.00001	0.00009	0.00036	0.00059
RFS_7	0.00079	0.00024	0.00047	0.00001	0.00035	0.00075	0.00101
RFS_8	0.00060	0.00011	0.00030	0.00014	0.00068	0.00109	0.00126

Table 6. RFS for the mesh size 1 mm

Scenario	1b	2b	3b	4b	5b	6b	7b
Damage location	24 mm	30 mm	36 mm	56 mm	73 mm	88 mm	97 mm
RFS_1	0.00307	0.00296	0.00301	0.00279	0.00265	0.00253	0.00246
RFS_2	0.00259	0.00227	0.00243	0.00178	0.00142	0.00113	0.00098
RFS_3	0.00218	0.00171	0.00194	0.00106	0.00063	0.00035	0.00022
RFS_4	0.00182	0.00124	0.00152	0.00054	0.00018	0.00004	0.00002
RFS_5	0.00146	0.00082	0.00112	0.00018	0.00000	0.00009	0.00022
RFS_6	0.00115	0.00051	0.00079	0.00001	0.00010	0.00041	0.00066
RFS_7	0.00089	0.00027	0.00054	0.00003	0.00038	0.00086	0.00112
RFS_8	0.00066	0.00012	0.00033	0.00017	0.00074	0.00123	0.00139

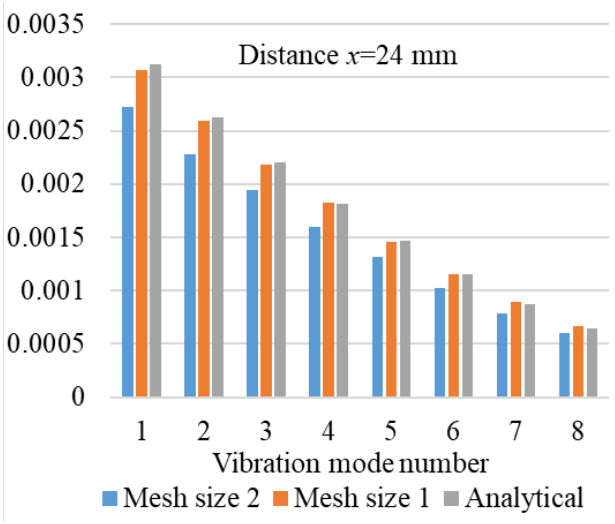

Figure 5. RFS comparison for crack position x = 24 mm

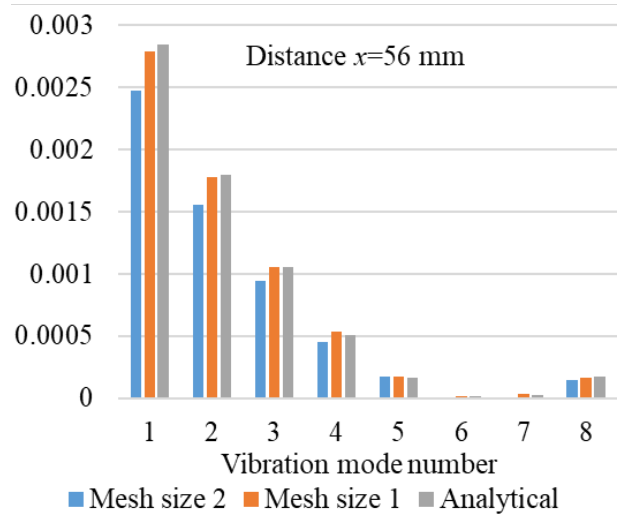

Figure 6. RFS comparison for crack position x = 56 mm

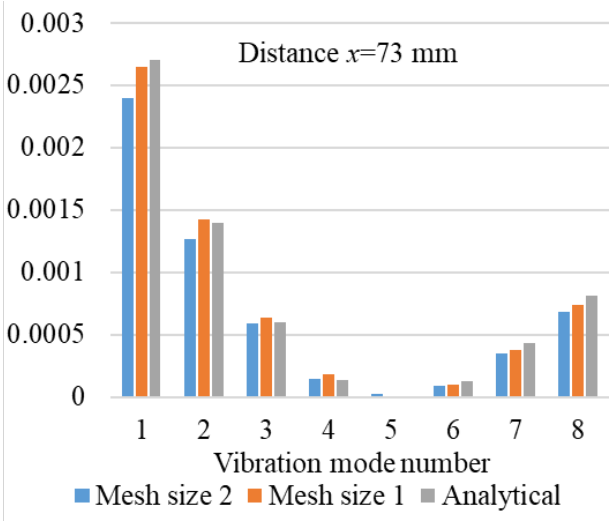

Figure 7. RFS comparison for crack position x = 73 mm

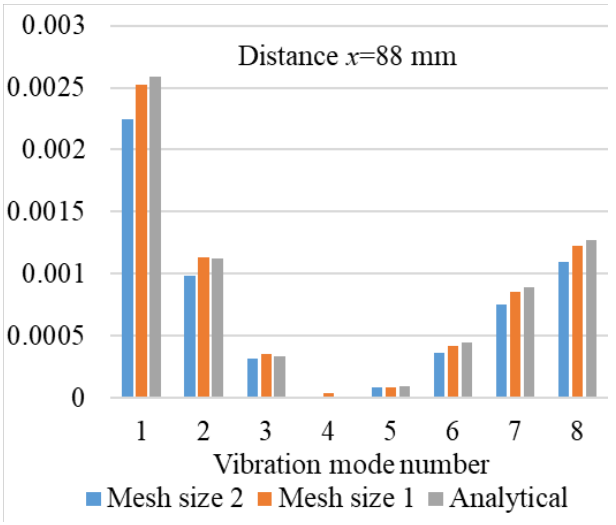

Figure 8. RFS comparison for crack position x = 88 mm

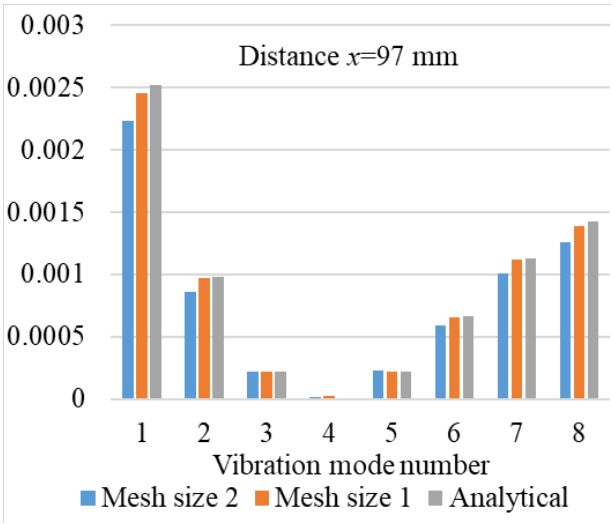

Figure 9. RFS comparison for crack position x = 97 mm

One can observe that the results obtained involving the FEM and fine mesh are closer to the values calculated with Eq. (4). However, the. models generated with a mesh size of 2 mm reflect the allure of the calculated RFS but indicate a smaller severity. From the illustrated comparison we can observe that the frequency shift due to a crack is small so in real-life applications, it is important to acquire the signals and estimate the frequencies with high precision. Advanced modal analysis techniques, like those presented in papers [20-22], should be considered.

5. RESULTS AND DISCUSSIONS

The validation is made by testing the RF models with RFS values obtained from the FEM simulation. The results are presented in Table 7 for the 2 mm mesh size and in Table 8 for the 1 mm mesh size.

Table 7. The RF models estimated crack positions for the obtained FEM RFS values using a 2 mm mesh size

Scenario	1a	2a	3a	4a	5a	6a	7a
Damage location [mm]	24	30	36	56	73	88	97
RF1 estimated location [mm]	14.25	39.04	24.25	51.22	72.55	88.6	87.3
RF1 error [%]	*0.98*	*0.30*	*0.58*	*0.48*	*0.05*	*0.06*	*0.97*
RF2 estimated location [mm]	15.29	39.09	24.37	52.02	72.57	88.32	86.07
RF2 error [%]	*0.87*	*0.31*	*0.56*	*0.40*	*0.04*	*0.03*	*1.09*
RF3 estimated location [mm]	25.41	40.49	32.28	57.68	74.52	90.14	91.92
RF3 error [%]	*0.14*	*0.45*	*0.23*	*0.17*	*0.15*	*0.21*	*0.51*
RF4 estimated location [mm]	23.48	36.31	27.35	55.03	72.51	89.63	91.69
RF4 error [%]	*0.05*	*0.03*	*0.27*	*0.10*	*0.05*	*0.16*	*0.53*

Table 8. The RF models estimated crack positions for the obtained FEM RFS values using a 1 mm mesh size

Scenario	1a	2a	3a	4a	5a	6a	7a
Damage location [mm]	24	30	36	56	73	88	97
RF1 estimated location [mm]	16.39	34.55	17.69	50.44	71.74	86.32	88.12
RF1 error [%]	*0.76*	*0.15*	*1.23*	*0.56*	*0.13*	*0.17*	*0.89*
RF2 estimated location [mm]	16.92	33.92	19.09	51.22	71.34	85.3	87.87
RF2 error [%]	*0.71*	*0.21*	*1.09*	*0.48*	*0.17*	*0.27*	*0.91*
RF3 estimated location [mm]	25.31	35.98	30.79	56.61	71.89	85.58	93.88
RF3 error [%]	*0.13*	*0.00*	*0.08*	*0.06*	*0.11*	*0.24*	*0.31*
RF4 estimated location [mm]	23.64	35.36	28.87	54.61	72.45	86.4	91.32
RF4 error [%]	*0.04*	*0.06*	*0.11*	*0.14*	*0.05*	*0.16*	*0.57*

The results presented in tables 7 and 8 are represented as diagrams in Figures 10 and 11 to facilitate an easy comparison. These show that for the RF1 and RF2, based on datasets with fewer data, the errors are bigger, irrespective of the mesh size used for FEM simulations. These errors are, however, less than 1.25%, which is quite remarkable.

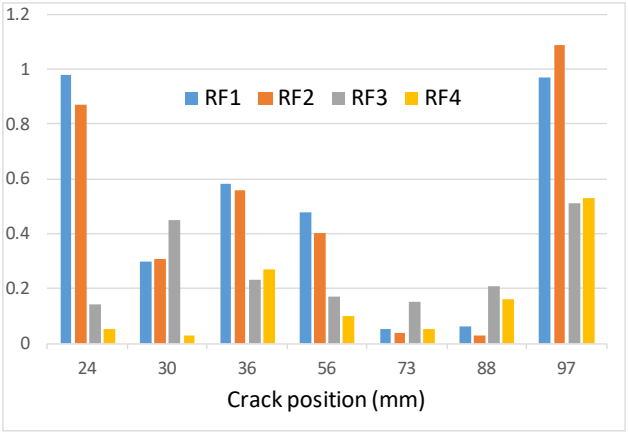

Figure 10. Error distribution for the coarse meshed beam

The most accurate results are obtained for the RF3 model when searching cracks in beams modeled with elements with the biggest edge of 1 mm. For this case, the maximum achieved error is 0.31%. Similarly, small errors are obtained with RF4, which has generally smaller errors, except for the crack position 97 mm. The precision obtained involving RF is better than that obtained with classical methods [23].

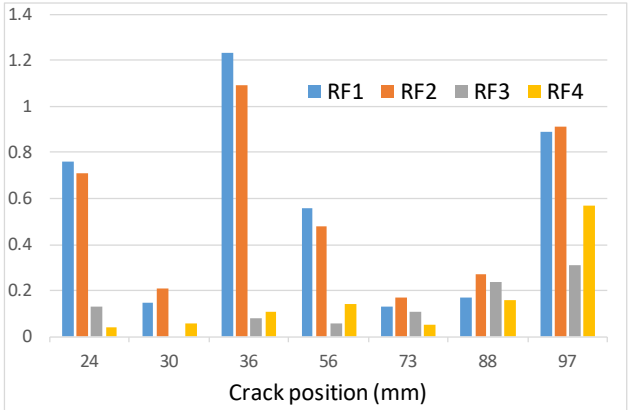

Figure 11. Error distribution for the beam with a fine mesh

The analysis revealed that the proposed method can detect the position of the damage even for noisy data, which is, in real-world applications unavoidable, despite the involvement of advanced frequency estimation techniques.

6. CONCLUSIONS

The paper presents a method to find the structural response for a multitude of damage scenarios. The response in terms of eigenfrequencies is used to create noise-free large datasets. These are used to train RF models able to detect transverse cracks in beam-like structures. In this study, we trained four RF models with a different number of data.

The models are trained for detecting the presence and location of damage that is situated in the area where high bending moments act of the cantilever beam and where is most susceptible to occur cracks. The accuracy of each damage detection model is determined by using the RFS values obtained from FEM analysis for different damage scenarios and mesh size parameters.

All four RF models were able to successfully indicate the crack location with high accuracy, even for the reduced resolution dataset. The maximum error achieved in locating cracks was 1.25%, the best model succeeds even to locate damage with the highest error of 0.03%. Better performance is achieved for the RF models that are trained using higher-resolution data, respectively RF3 and RF4.

ACKNOWLEDGMENTS

This paper received financial support through the project "Entrepreneurship for innovation through doctoral and postdoctoral research": POCU/380/ 6/13/123866, a project co-financed by the European Social Fund through the Operational Program Human Capital 2014-2020.

REFERENCES

[1] Doebling S.W., Farrar C., Prime M.B., Shevitz D.W., Damage Identification and Health Monitoring of Structural and Mechanical Systems from Changes in their Vibration Characteristics: A Literature Review, *Shock and Vibration Digest*, Vol. 30, 1996, Art.No. 11, DOI: 10.2172/249299.

[2] Bovsunovsky A., Surace C., Structural damage detection based on features insensitive to ambient factors, *Theoretical and applied fracture mechanics*, Vol. 110, 2020, Art.Nuo. 102780, DOI: 10.1016/j.tafmec.2020.102780.

[3] Yang Y., Zhang Y., Tan XK., Review on Vibration-Based Structural Health Monitoring Techniques and Technical Codes, *Symmetry-Basel*, Vol.13, No.11, 2021, Art.No.1998.

[4] Sha G.G., Cao M.S., Radzienscki M., Ostachowicz W., Delamination-induced relative natural frequency change curve and its use for delamination localization in laminated composite beams, *Composite Structures*, Vol. 230, 2019, Art.No. 111501, DOI: 10.1016/j.compstruct.2019.111501.

[5] Stoykov S., Manoach E., Damage localization of beams based on measured forced responses, *Mechanical Systems and Signal Processing*, Vol. 151, 2021, Art.No. 107379, DOI: 10.1016/j.ymssp.2020.107379.

[6] OBrien E.J., Malekjafarian A., A mode shape-based damage detection approach using laser measurement from a vehicle crossing a simply supported bridge, *Structural Control and Health Monitoring*, Vol. 23, No. 10, 2016, pp. 1273-1286, DOI: 10.1002/stc.1841.

[7] Caicedo D., Lara-Valencia L.A., Brito J., Frequency-based methods for the detection of damage in structures: A chronological review, *DYNA*, Vol. 88, No. 218, 2021, pp. 203-211, DOI: 10.15446/dyna. v88n218.91693.

[8] Tran-Ngoc H., Khatir S., Wahab M.A., Efficient Artificial neural networks based on a hybrid metaheuristic optimization algorithm for damage detection in laminated composite structures, *Composite Structures,* Vol. 262, 2021, Art.No. 113339, DOI: 10.1016/j.compstruct.2020.113339.

[9] Meriem S., Djamel N., Djilali B., Khatir S., Wahab M.A., Crack prediction in beam-like structure using ANN based on frequency analysis, *Frattura ed Integrità Strutturale*, Vol. 59, 2022, pp. 18-34, DOI: 10.3221/IGF-ESIS.59.02.

[10] Nguyen Q.T., Livaoglu R., Combination of an inverse solution and an ANN for damage identification on high-rise buildings, *Smart Structures and Systems*, Vol. 28, No. 3, 2021, pp. 375-390.

[11] Tufisi C., Gillich N., Gillich G.R., A Cost Function to Assess Cracks in Simply Supported Beams with Artificial Intelligence, *Romanian Journal of Acoustics and Vibration,* Vol. 18, No. 1, 2021, pp.46-52.

[12] T Sang-To H., Le-Minh T.T., Danh S., Khatir M., Wahab M.A., Cuong-Le T., Combination of Intermittent Search Strategy and an Improve Particle Swarm Optimization algorithm (IPSO) for model updating, *Frattura ed Integrità Strutturale*, Vol. 59, 2022, pp. 141-152, DOI:10.3221/IGF-ESIS.59.11.

[13] Mariniello G., Patore T., Menna C., Festa P., Asprone D., Structural damage detection and localization using decision tree ensemble and vibration data, *Computer-Aided Civil and Infrastructure Engineering*, Vol. 36, No. 9, 2021, pp. 1129-1149.

[14] Guo G., Cui X., Du B., Random-Forest Machine Learning Approach for High-Speed Railway Track Slab Deformation Identification Using Track-Side Vibration Monitoring, *Computer-Aided Civil and Infrastructure Engineering*, Appl. Sci. 2021, Vol. 11, Art.No. 4756.

[15] Gillich G.R., Praisach Z.I., Modal identification and damage detection in beam-like structures using the power spectrum and time-frequency analysis. Signal Processing 2014, Vol. 96, pp. 29-44. DOI: 10.1016/j.sigpro.2013.04.027

[16] Gillich G.R., Wahab M.A., Praisach Z.I., Ntakpe J.L., The influence of transversal crack geometry on the frequency changes of beams, *Proceedings of International Conference on Noise and Vibration Engineering*, *and International Conference on Uncertainty in Structural Dynamics*, 2014, pp. 485–498.

[17] Gillich, N.; Tufisi, C.; Vasile, O.; Gillich, GR. Statistical Method for Damage Severity and Frequency Drop Estimation for a Cracked Beam using Static Test Data. *Romanian Journal of Acoustics and Vibration*, 2019, 16(1), 47-51.

[18] Gillich G.R., Birdeanu E.D., Gillich N., Amariei D., Iancu V., Jurcau C.S., Detection of damages in simple elements, *Annals of DAAAM & Proceedings*, 2009, pp. 623+.

[19] Probst P., Boulesteix A.L., To tune or not to tune the number of trees in random forest, *Journal of Machine Learning Research*, Vol. 18, No. 1, 2017, pp. 6673-6690.

[20] Gillich G.R., Mituletu I.C., Praisach Z.I., Negru I., Tufoi M., Method to Enhance the Frequency Readability for Detecting Incipient Structural Damage, *Iranian Journal of Science and Technology, Transactions of Mechanical Engineering*, Vol. 41, 2017, pp. 233–242, D OI: 10.1007/s40997-016-0059-8.

[21] Mituletu I.C., Gillich G.R., Maia N.M.M., A method for an accurate estimation of natural frequencies using swept-sine acoustic excitation, *Mechanical Systems and Signal Processing*, Vol. 116, 2019, pp. 693-709.

[22] Ntakpe J.L, Gillich G.R., Mituletu I.C., Praisach Z.I., Gillich N., An Accurate Frequency Estimation Algorithm with Application in Modal Analysis, *Romanian Journal of Acoustics and Vibration*, Vol. 13, No. 2, 2016, pp. 98-103.

[23] Minda P.F., Praisach Z.I., Gillich N., Minda A.A., Gillich G.R., On the efficiency of different dissimilarity estimators used in damage detection, *Romanian Journal of Acoustics and Vibration*, Vol. 10, No. 1, 2013, pp. 15-18.